Research Square

Preprints are preliminary reports that have not undergone peer review.
They should not be considered conclusive, used to inform clinical practice,
or referenced by the media as validated information.

Incremental prognostic value of baseline ^{18}F-FDG PET/CT tumour asphericity in breast carcinoma: association with de novo metastatic disease and survival outcomes

Nitin Gupta

nittinplp@gmail.com

Dr RPGMC Tanda Kangra https://orcid.org/0000-0002-9443-9609

Research Article

Keywords: 18F-FDG PET/CT, breast cancer, tumour asphericity, metabolic tumour volume, total lesion glycolysis, metastasis, progression free survival, overall survival

Posted Date: April 1st, 2026

DOI: https://doi.org/10.21203/rs.3.rs-9221004/v1

License: This work is licensed under a Creative Commons Attribution 4.0 International License.
Read Full License

Additional Declarations: The authors declare no competing interests.

Abstract

Background

Tumour asphericity (ASP), derived from baseline 18F-FDG PET/CT, may capture morphologic heterogeneity linked to aggressive biology and adverse outcomes.

Aim

To evaluate the incremental value of baseline ASP for de novo metastatic disease at presentation and survival outcomes in breast carcinoma beyond clinical stage, receptor-derived subtype, Ki-67 and metabolic tumour burden.

Methods

Patient-level data (n = 180) were analysed. De novo metastasis (stage IV) was modelled using multivariable logistic regression with 5-fold cross-validated ROC analysis; model calibration was assessed using observed versus predicted risk. PFS and OS were analysed using Kaplan-Meier, log-rank tests and multivariable Cox proportional hazards regression.

Results

De novo metastatic disease was present in 37/180 patients (20.6%). In multivariable logistic regression, ASP (per 0.1 increase) independently predicted baseline metastasis (OR 3.60, 95% CI 2.02 to 6.43, $p < 0.001$) along with ln(TLG) (natural logarithm transformed TLG; OR 2.47, 95% CI 1.32 to 4.63, $p = 0.0047$). Out-of-fold AUC for metastasis prediction was 0.80 for ASP alone and 0.82 for the full model including ASP; calibration was satisfactory (calibration slope 1.00; Brier score 0.117). Higher ASP was also associated with treatment non-response (OR 1.99 per 0.1, $p = 0.00033$). On unadjusted analysis over full follow-up (not administratively censored), ASP > 0.30 (vs ASP ≤ 0.30) was associated with shorter PFS (median 24.7 vs 9.6 months; log-rank $p = 0.0017$) and OS (median 28.2 vs 10.8 months; log-rank $p = 0.00011$).

Conclusion

Baseline tumour asphericity derived from ^{18}F-FDG PET/CT is a simple, interpretable geometric biomarker that outperforms conventional metabolic indices and biomarker variables for baseline metastasis discrimination and is associated with treatment non-response and shorter median PFS and OS on unadjusted survival analysis. Prospective multicentre validation is warranted.

Introduction

Breast cancer remains the most commonly diagnosed malignancy worldwide and a leading cause of cancer related mortality[1]. Although major therapeutic advances have improved outcomes, distant metastasis and treatment resistance continue to drive breast cancer deaths [2]. Baseline staging is therefore essential to guide treatment selection and prognostication, with whole body ^{18}F-FDG PET/CT increasingly used in clinically high risk patients to detect extra axillary nodal and distant metastases and to establish a quantitative baseline for response assessment[3, 4]. Beyond detection of overt metastatic disease, baseline PET/CT metrics may help contextualize tumour biology across molecular subtypes and inform risk-adapted systemic and locoregional strategies [2, 4] .

Robust quantification depends on harmonized acquisition, reconstruction and reporting as emphasized by contemporary procedure guidelines[5]. Conventional PET biomarkers such as SUVmax, metabolic tumour volume (MTV) and total lesion glycolysis (TLG) reflect uptake intensity and tumour burden; meta-analytic evidence supports their prognostic association in breast cancer, but clinically meaningful overlap persists among patients with similar clinicopathologic features[6]. Treatment response frameworks including the EORTC recommendations and PERCIST summarize response largely through uptake based measures [7, 8]. Radiomics expands quantitative imaging by extracting descriptors of intensity, texture and geometry that may capture tumour phenotype and microenvironment [9, 10, 11]. and standardization initiatives such as the Image Biomarker Standardisation Initiative (IBSI) provide consensus definitions to improve reproducibility[12]. Among radiomic feature families, shape metrics are intuitive and comparatively less dependent on intensity normalization; asphericity (ASP = 1 - sphericity) summarizes deviation from a sphere and has shown independent prognostic value in other FDG avid cancers beyond conventional metabolic indices[13, 14]. In breast cancer, PET derived radiomic indices including texture features have been linked to outcome, but the incremental value of primary tumour asphericity in routine clinical cohorts remains incompletely defined[15]. Because ASP is derived from surface area and volume, it is readily computable from standard tumour VOIs and is potentially amenable to routine reporting when robust segmentation is available.

This study aimed to evaluate the prognostic and predictive utility of baseline ^{18}F-FDG PET/CT tumour asphericity (ASP) for baseline distant metastasis, progression free survival (PFS) and overall survival (OS) in breast carcinoma, and to determine whether ASP provides incremental value beyond clinical stage, molecular receptor status (ER/PR/HER2), Ki-67 and standard metabolic tumour burden metrics (SUVmax, MTV and TLG). We also compared the discriminative performance of ASP against metabolic and biomarker variables for metastasis prediction and assessed its contribution in multivariable survival models.

Why this matters clinically

Early risk stratification is central to treatment selection and counselling in breast carcinoma [2]. Patients presenting with occult metastatic disease often require systemic therapy rather than curative local approaches, and those at high risk of early progression may benefit from intensified therapy and closer surveillance. Baseline distant staging investigations are generally reserved for higher risk presentations[3] and ^{18}F-FDG PET/CT can upstage disease and inform management in intermediate and high risk cohort[4]. If a simple PET derived morphologic metric such as ASP can help identify patients more likely to harbour metastatic disease at diagnosis or experience early events, it could complement staging and metabolic burden measures without additional cost or radiation exposure.

Materials and methods

Study design and cohort

This retrospective patient level dataset included 180 patients with breast carcinoma who underwent baseline ^{18}F-FDG PET/CT prior to definitive therapy. Clinical stage (I to IV), histologic grade (I to III), receptor derived subtype (HR+/HER2+, HR+/HER2-, HR-/HER2+, TNBC), Ki-67 category, and treatment variables (neoadjuvant chemotherapy [NACT], surgery, radiotherapy [RT]) were recorded. ER, PR, HER2 and Ki-67 status were extracted from pathology reports and recorded as binary categories; receptor derived subtype was constructed from hormone receptor status (ER or PR) and HER2 status.

PET/CT acquisition and reconstruction parameters

All studies were acquired on a GE Discovery IQ 610 (32 slice) hybrid PET/CT system (GE Healthcare, Waukesha, WI, USA). Patients received ~ 3.7 MBq/kg of ^{18}F-FDG, and imaging was performed after an uptake time of 60 ± 10 minutes. Whole body PET emission data were acquired in 3D mode using a multi bed position protocol (2 minutes per bed position) with bed overlap as per institutional protocol. PET images used for analysis were reconstructed using Q.Clear (BSREM; DICOM reconstruction method QCHD) with CT based attenuation correction, on a 192 × 192 matrix with voxel size 3.65 × 3.65 × 3.23 mm (reconstruction diameter 700 mm). Low dose CT for attenuation correction and anatomical localization was performed at 120 kVp with automatic tube current modulation, reconstructed at 512 × 512 with 0.85 × 0.85 mm in plane pixel spacing and 1.25 mm slice thickness (pitch 0.9375, rotation time 0.7 s; reconstruction diameter 434 mm). Multiplanar reformats (axial, coronal, sagittal) were generated on the workstation.

Image analysis and tumour segmentation

Primary breast tumour volumes of interest were delineated on baseline PET/CT using a standardised semi-automated workflow with manual refinement and consensus review by two experienced nuclear medicine physicians. To minimise spill-in from physiologic uptake and nodal disease, automated organ

and axillary nodal masks generated using TotalSegmentator and an nnU-Net model were used as exclusion priors during contour refinement.

Surface mesh extraction and tumor asphericity calculation

Tumour sphericity and asphericity were derived from surface area and volume of the segmented primary tumour. Masks were resampled to an isotropic grid for shape analysis and a triangular surface mesh was extracted using Marching cubes. Volume (V) and surface area (A) were computed from the mesh and sphericity (Psi) was calculated as Psi = pi^(1/3) * (6V)^(2/3) / A; asphericity was defined as ASP = 1 - Psi. For modelling, ASP was analysed as a continuous variable (per 0.1 increase) and for Kaplan-Meier analyses patients were dichotomised at the prespecified cut off (0.30).

Quantitative metabolic PET metrics

SUV based metrics were computed from the native resolution PET image using scanner DICOM metadata for injected dose and patient weight (body weight normalised SUV). Within the primary tumour VOI, SUVmax, metabolic tumour volume (MTV, mL) and total lesion glycolysis (TLG, g) were derived using standard definitions.

Endpoints

Treatment response was available as a binary variable indicating non-response at the first post treatment assessment. Non-response was defined as absence of an objective response at the first post treatment evaluation as captured in the dataset; because detailed response criteria were not uniformly documented, this endpoint was analysed as exploratory.

De novo metastatic disease was defined as stage IV at presentation. Progression free survival (PFS) was defined as time from baseline PET/CT to documented progression or death; overall survival (OS) was defined as time from baseline PET/CT to death from any cause. Patients without an event were administratively censored at last follow up (maximum 84 months).

Baseline metastasis was modelled using multivariable logistic regression. Predictive performance was assessed using stratified five-fold cross-validated ROC analysis with out of fold AUC reporting. Model calibration was evaluated using calibration in the large and calibration slope, and by plotting observed versus predicted risk across deciles. To quantify potential optimism in discrimination metrics, bootstrap resampling (300 resamples) was used to derive optimism corrected AUC estimates. PFS and OS were analysed using Kaplan-Meier methods with log-rank testing for ASP groups (cut off 0.30), and using Cox proportional hazards regression. The ASP dichotomisation threshold of 0.30 was selected as a rounded, clinically interpretable value anchored to the cohort specific ROC Youden cut point for baseline metastasis (approximately 0.287) and was then applied consistently across treatment response and survival analyses rather than re optimising a separate threshold for each endpoint. Primary multivariable

Cox models included baseline covariates only; recorded treatment variables were evaluated in exploratory analyses and interpreted cautiously because treatments may occur after baseline PET/CT. Because SUVmax, MTV and TLG are correlated measures of metabolic tumour activity, multivariable models used ln(TLG) as the representative metabolic burden variable; ln(SUVmax) and ln(MTV) were evaluated in separate sensitivity analyses and for univariable discrimination. Sensitivity prognostic analyses were additionally performed in patients with stage I to III disease only, with stage modelled as a categorical variable. To assess incremental value of ASP, nested model likelihood ratio tests compared models with and without ASP. All tests were two sided with $p < 0.05$ considered statistically significant. Clinical utility of baseline metastasis prediction models was assessed using decision curve analysis, estimating net benefit across threshold probabilities from 0.05 to 0.60 and comparing model based strategies with treat all and treat none approaches[20]. Natural logarithm transformation was applied to SUVmax, MTV and TLG for regression modelling; ln denotes natural logarithm.

Results

Cohort characteristics

The analysis included 180 patients (mean age 51.6 ± 11.4 years). Stage distribution was stage I (n = 8 ~ 4.4%), II (n = 74 ~ 41.1%), III (n = 61 ~ 33.9%), and stage IV (n = 37 ~ 20.6%). Receptor derived subtypes were HR+/HER2- (n = 99), TNBC (n = 41), HR-/HER2+ (n = 24), and HR+/HER2+ (n = 16). De novo metastatic disease was present in 37 patients (20.6%).

In multivariable logistic regression including age, grade, Ki-67, subtype and ln(TLG), ASP remained an independent predictor of baseline metastasis. ASP (per 0.1 increase) showed OR 3.60 (95% CI 2.02 to 6.43; $p < 0.001$). ln(TLG) (natural logarithm transformed TLG) was also independently associated with metastasis (OR 2.47; 95% CI 1.32 to 4.63; $p = 0.0047$). Adding ASP significantly improved model fit compared with the same covariates without ASP (likelihood ratio $p < 0.00001$). Out of fold AUCs were 0.80 (ASP only), 0.71 (metabolic only), 0.62 (clinical only) and 0.82 (full model). Calibration was acceptable (calibration intercept 0.00; calibration slope 1.00; Brier score 0.117) and is shown in Supplementary Figures S3 and S4. The apparent AUC of the full model was 0.85 and the bootstrap optimism-corrected AUC was 0.81. ROC analysis of ASP alone for baseline metastasis yielded an AUC of 0.804 and identified an optimal cut point of 0.287 by the Youden method (sensitivity 86.5%, specificity 65.7%; Supplementary Figure S5). For clinical interpretability, a rounded cut off of 0.30 was used for Kaplan-Meier stratification.

Survival outcomes

Kaplan-Meier survival analyses stratified by baseline tumour asphericity using the prespecified cut off (ASP > 0.30 vs ASP ≤ 0.30) demonstrated significantly inferior outcomes in the high asphericity group in the overall cohort (Fig. 3), with median overall survival 10.8 months for ASP > 0.30 (n = 71) versus 28.2 months for ASP ≤ 0.30 (n = 109) (log-rank $p = 0.00016$) and median progression free survival 9.6 versus 24.7 months (log-rank $p = 0.0030$), with curves administratively censored at 60 months. On molecular

subtype stratified analysis (Fig. 4), overall survival remained significantly worse with high asphericity in HR+/HER2- (9.7 vs 27.9 months; p = 0.0025) and TNBC (15.1 vs 47.6 months; p = 0.0348), but not in HER2 + disease (10.7 vs 21.3 months; p = 0.268). For progression free survival, high asphericity was associated with shorter PFS in HR+/HER2− (17.4 vs 32.8 months; p = 0.00069), whereas no significant separation was observed in HER2+ (8.8 vs 4.7 months; p = 0.861) or TNBC (4.1 vs 17.7 months; p = 0.932). Separate overall cohort Kaplan-Meier plots for PFS and OS over full follow up are provided as Supplementary Figures S1 and S2.

After adjustment for age, clinical stage, grade, subtype, Ki-67 and ln(TLG) in multivariable Cox models, ASP was not independently associated with PFS or OS. For PFS, stage was the dominant predictor (HR 1.86 per stage increment; p < 0.001), and the incremental contribution of ASP was not significant (likelihood ratio p = 0.743). For OS, stage remained the dominant predictor (HR 1.94 per stage increment; p < 0.001), and adding ASP to the clinical plus metabolic model did not improve fit (likelihood ratio p = 0.909). In sensitivity analyses restricted to stage I to III disease with stage modelled categorically, stage III (vs stage I and II) remained associated with shorter PFS (HR 1.69; p = 0.031) and showed a similar trend for OS (HR 1.59; p = 0.077), whereas ASP was not associated with PFS (HR 1.01 per 0.1; p = 0.923) or OS (HR 1.02 per 0.1; p = 0.898).

Comparative performance across imaging, clinicopathologic, and biomarker variables is summarised in Figs. 5 and 6. For baseline metastasis discrimination, ASP provided the highest single variable AUC (0.80), exceeding ln(SUVmax) (0.72), ln(TLG) (0.71), ln(MTV) (0.67) and receptor or Ki-67 variables (AUC ≤ 0.58). For treatment non response, stage (AUC 0.71) and ln(SUVmax) (AUC 0.70) were the strongest discriminators, with ASP showing moderate discrimination (AUC 0.66). For time to event outcomes, stage had the highest Harrell's C for both PFS and OS (0.62 each); among imaging and biomarker variables, ASP had the highest C index (PFS 0.58; OS 0.59) and was associated with higher odds of baseline metastasis (OR 3.70 per 0.1, 95% CI 2.16 to 6.33) and shorter PFS (HR 1.37 per 0.1, 95% CI 1.15 to 1.62) and OS (HR 1.33 per 0.1, 95% CI 1.12 to 1.58).

Tables

Table 1

Baseline clinicopathologic, treatment, and PET derived tumour characteristics of the study cohort. Continuous variables are presented as mean ± standard deviation or median (interquartile range), as appropriate; categorical variables are presented as n (%). Hormone receptor status and HER2 status are based on standard immunohistochemistry reporting; Ki-67 is reported as percentage

Variable	Overall	Non-metastatic (stage I–III)	Metastatic (stage IV)
Age	51.6 ± 11.4	52.2 ± 11.1	49.4 ± 12.0
SUVmax	14.1 ± 6.8	13.2 ± 6.6	17.7 ± 6.7
MTV_ml	23.5 ± 22.8	22.3 ± 23.9	28.5 ± 17.2
TLG_g	185.1 ± 169.0	165.9 ± 154.0	259.0 ± 203.5
ASP	0.3 ± 0.1	0.3 ± 0.1	0.3 ± 0.1
PFS_months	26.4 ± 25.6	30.4 ± 26.6	11.2 ± 12.7
OS_months	34.0 ± 31.7	39.5 ± 32.4	12.7 ± 16.2
Stage: I	8 (4.4%)	8 (5.6%)	0 (0.0%)
Stage: II	74 (41.1%)	74 (51.7%)	0 (0.0%)
Stage: III	61 (33.9%)	61 (42.7%)	0 (0.0%)
Stage: IV	37 (20.6%)	0 (0.0%)	37 (100.0%)
Grade: I	26 (14.4%)	19 (13.3%)	7 (18.9%)
Grade: II	80 (44.4%)	63 (44.1%)	17 (45.9%)
Grade: III	74 (41.1%)	61 (42.7%)	13 (35.1%)
Subtype_derived: HR+/HER2+	16 (8.9%)	10 (7.0%)	6 (16.2%)
Subtype_derived: HR+/HER2-	99 (55.0%)	85 (59.4%)	14 (37.8%)
Subtype_derived: HR-/HER2+	24 (13.3%)	17 (11.9%)	7 (18.9%)
Subtype_derived: TNBC	41 (22.8%)	31 (21.7%)	10 (27.0%)
Ki67_high: 0	85 (47.2%)	65 (45.5%)	20 (54.1%)
Ki67_high: 1	95 (52.8%)	78 (54.5%)	17 (45.9%)
NACT: 0	49 (27.2%)	48 (33.6%)	1 (2.7%)
NACT: 1	131 (72.8%)	95 (66.4%)	36 (97.3%)
Surgery_any: 0	26 (14.4%)	0 (0.0%)	26 (70.3%)
Surgery_any: 1	154 (85.6%)	143 (100.0%)	11 (29.7%)

Variable	Overall	Non-metastatic (stage I–III)	Metastatic (stage IV)
RT: 0	38 (21.1%)	19 (13.3%)	19 (51.4%)
RT: 1	142 (78.9%)	124 (86.7%)	18 (48.6%)

Table 2

Univariable and multivariable logistic regression for predictors of baseline distant metastasis at presentation. Odds ratios (ORs) are reported with 95% confidence intervals (CI). PET metabolic variables were natural-log transformed (ln) where specified. The multivariable model used a collinearity-safe metabolic burden representation (ln[TLG]) and included tumour asphericity (ASP) to evaluate incremental value beyond clinicopathologic factors.

Predictor	OR	95% CI	p-value	Notes
Subtype: HR+/HER2-	0.35	0.09 to 1.40	0.137	
Subtype: HR-/HER2+	1.19	0.24 to 5.94	0.836	
Subtype: TNBC	1.09	0.26 to 4.56	0.910	
ASP (per 0.1)	3.60	2.02 to 6.43	< 0.001	
ln(TLG)	2.47	1.32 to 4.63	0.0047	
Age	0.98	0.95 to 1.02	0.403	
Grade (per level)	0.87	0.47 to 1.62	0.664	
Ki-67 high	0.38	0.14 to 1.02	0.054	

Table 3

Multivariable Cox proportional hazards regression for progression-free survival. Hazard ratios (HRs) are reported with 95% confidence intervals (CI). PET metabolic variables were natural-log transformed (ln) where specified. Baseline covariates were used for the primary Cox model; treatment variables were evaluated in exploratory analyses and interpreted cautiously.

Predictor	HR	95% CI	p-value
Age	1.01	0.99 to 1.02	0.218
Stage (per increment)	1.86	1.42 to 2.45	< 0.001
Grade (per level)	1.05	0.85 to 1.31	0.624
Ki-67 high	1.24	0.88 to 1.75	0.219
ln(TLG)	1.10	0.93 to 1.29	0.270
ASP (per 0.1)	0.96	0.76 to 1.21	0.743
Subtype: HR+/HER2-	0.81	0.46 to 1.46	0.490
Subtype: HR-/HER2+	1.01	0.52 to 1.95	0.981
Subtype: TNBC	0.93	0.51 to 1.71	0.825

Table 4
Multivariable Cox proportional hazards regression for overall survival. Hazard ratios (HRs) are reported with 95% confidence intervals (CI). PET metabolic variables were natural-log transformed (ln) where specified. Baseline covariates were used for the primary Cox model; treatment variables were evaluated in exploratory analyses and interpreted cautiously.

Predictor	HR	95% CI	p-value
Age	1.01	1.00 to 1.03	0.085
Stage (per increment)	1.94	1.46 to 2.59	< 0.001
Grade (per level)	1.26	0.98 to 1.61	0.075
Ki-67 high	1.13	0.77 to 1.64	0.539
ln(TLG)	1.08	0.89 to 1.30	0.428
ASP (per 0.1)	0.99	0.78 to 1.24	0.909
Subtype: HR+/HER2-	1.47	0.79 to 2.76	0.226
Subtype: HR-/HER2+	1.23	0.60 to 2.52	0.570
Subtype: TNBC	0.96	0.49 to 1.89	0.913
Figures and legends			

Discussion

In our study, baseline tumour asphericity (ASP) was strongly associated with baseline distant metastasis and with shorter PFS and OS on univariable analyses. Notably, ASP provided the strongest single imaging discriminator for baseline metastasis compared with conventional metabolic parameters (SUVmax, MTV and TLG) and biomarker variables, supporting ASP as a compact descriptor of tumour aggressiveness that is not captured by burden metrics alone. For survival endpoints, clinical stage remained the dominant determinant, and ASP did not retain independent prognostic significance after adjustment, suggesting that ASP largely reflects (or co-segregates with) advanced disease extent at presentation. These observations are consistent with biological frameworks that link tumour heterogeneity to acquisition of invasive and metastatic capabilities and microenvironmental pressures such as hypoxia[18, 19].

For dichotomised Kaplan-Meier analyses we used ASP 0.30 (ASP > 0.30 vs ASP ≤ 0.30) as a clinically interpretable threshold. This value was not arbitrarily selected, but was anchored to the cohort specific ROC derived Youden cut point for baseline metastasis (0.287; Supplementary Figure S5) and rounded for practical application. ASP remained modelled as a continuous variable in the primary regression analyses, which reduces information loss and limits threshold driven overfitting.

From a clinical utility perspective, decision curve analysis indicated that adding ASP to the metastasis prediction model increases net benefit over clinically relevant threshold probabilities, outperforming treat-all and models based on clinical and metabolic burden alone[20] (Fig. 7). If externally validated, an ASP augmented risk model could support risk adapted selection of patients for intensified metastatic work up (or referral for systemic therapy pathways) in settings where whole body PET/CT is not routinely performed for all presentations, without materially increasing the burden of false positive escalation.

Beyond baseline metastasis discrimination, baseline tumour asphericity also carried clinically relevant information regarding treatment response. In our cohort, asphericity was associated with higher odds of treatment non response (OR 1.99 per 0.1 increase; p = 0.00033) and provided moderate discrimination for non response (AUC 0.66), comparable to conventional baseline indices such as SUVmax and stage (Figs. 5 and 6). This is consistent with prior breast cancer FDG PET evidence that pretreatment imaging phenotype and early treatment related changes can identify patients at risk of suboptimal response and relapse, and with PET/CT radiomics studies in which pretreatment feature signatures predicted pathological response to neoadjuvant chemotherapy and subsequent outcomes[21, 22, 23, 24, 25]. A systematic review and meta-analysis supports the prognostic value of FDG PET based response assessment after neoadjuvant chemotherapy in breast cancer[29].

For survival, higher baseline asphericity (ASP > 0.30) was associated with substantially shorter median overall survival (10.8 vs 28.2 months) and median progression free survival (9.6 vs 24.7 months), and these separations remained evident within molecular subtypes in Kaplan-Meier analyses (Figs. 3 and 4). However, these Kaplan-Meier comparisons were unadjusted, and ASP did not remain independently associated with PFS or OS after adjustment for stage, grade, subtype, Ki-67 and ln(TLG) in the multivariable Cox models. This pattern suggests that ASP captures an adverse baseline phenotype and disease extent that is clinically useful for risk stratification, while the dominant adjusted survival signal in this cohort was carried by stage. Prior breast cancer and broader FDG PET studies have reported prognostic associations of pretreatment asphericity and other heterogeneity features, including independent effects in some cohorts, whereas attenuation after adjustment for stage or tumour burden has also been observed depending on cohort composition, endpoint definition and model specification[13, 14, 26, 27, 28].

These findings are concordant with prior breast cancer literature demonstrating prognostic relevance of metabolic tumour burden and PET derived heterogeneity. Meta-analyses support MTV and TLG as prognostic biomarkers in breast cancer, although their incremental value can vary by subtype and stage[6, 9, 10, 11, 12]. In ER+/HER2- tumours, Groheux and colleagues showed that baseline FDG PET indices have prognostic value, with MTV remaining significant after multivariable adjustment while textural analysis did not add beyond volume measures[15]. Our results complement these observations by showing that a simple geometric descriptor of FDG uptake, tumour asphericity, captures spatial irregularity distinct from tumour burden, is strongly linked to metastatic presentation and treatment non

response, and provides clear unadjusted survival stratification even when stage dominates multivariable Cox models.

From a biological standpoint, irregular tumour geometry may reflect infiltrative growth, heterogeneous proliferation, angiogenesis and hypoxia driven selection of aggressive subclones. Hypoxia inducible signalling has been linked to invasion, metastatic dissemination and treatment resistance[18], consistent with hallmark mechanisms of cancer progression[19]. In line with this paradigm, asphericity has shown independent prognostic associations in several FDG avid tumours, including NSCLC and head and neck cancer [13, 14], and more recently in cervical cancer and in a multicentre head and neck cohort[27, 28], supporting generalizability of shape derived risk signals across tumour types. Taken together, baseline tumour asphericity is an interpretable PET derived biomarker that complements stage and conventional metabolic parameters, with value for baseline metastatic risk, treatment non response, and unadjusted survival stratification. In our cohort, the survival association of ASP was substantially attenuated after multivariable adjustment, indicating that its prognostic signal is closely intertwined with disease stage and extent at presentation. Incorporating asphericity into multiparametric baseline models alongside stage, subtype and treatment may still help identify high risk patients who could benefit from intensified systemic therapy, closer surveillance or clinical trial enrolment.

Limitations of the study

Limitations of the present study include the retrospective design, heterogeneous treatments, and incomplete or non standardized response assessment in some patients. Additionally, asphericity depends on lesion segmentation and can be influenced by image reconstruction, partial volume effects and thresholding. While we applied harmonized workflows and quality control, prospective multicentre validation with standardized response criteria and external calibration of ASP thresholds is needed before routine clinical adoption. A large proportion of patients received neoadjuvant chemotherapy, and primary treatment approach is closely linked to stage and tumour biology; therefore treatment heterogeneity may confound associations with survival and response. In exploratory sensitivity Cox models that additionally adjusted for baseline NACT status, the stage dominant results were unchanged and ASP remained not independently associated with PFS or OS (data not shown).

Conclusion

Baseline tumour asphericity derived from ^{18}F-FDG PET/CT is a simple, interpretable marker of tumour geometry and heterogeneity that outperforms conventional metabolic indices and biomarker variables for baseline metastasis discrimination. Higher baseline asphericity was also associated with a higher likelihood of treatment non response and with substantially shorter median PFS and OS on Kaplan-Meier analysis, supporting its utility for baseline risk stratification and clinical communication. However, ASP did not retain independent significance for PFS or OS after adjustment for stage and other baseline covariates in multivariable Cox models in this cohort. Prospective, multicentre validation is warranted.

Declarations

Funding: None.

Conflicts of interest: The authors declare no competing interests.

Ethics approval: This retrospective analysis was approved by the Institutional Ethics Committee of Dr Rajendra Prasad Government Medical College, Kangra, Himachal Pradesh, and the requirement for informed consent was waived.

Data availability: De-identified data supporting the findings are available from the corresponding author on reasonable request.

References

1. Sung H, Ferlay J, Siegel RL et al (2021) Global cancer statistics 2020: GLOBOCAN estimates of incidence and mortality worldwide for 36 cancers in 185 countries. CA Cancer J Clin 71(3):209–249. 10.3322/caac.21660PMID:33538338
2. Waks AG, Winer EP (2019) Breast Cancer Treatment: A Review. JAMA. ;321(3):288–300. 10.1001/jama.2018.19323. PMID:30667505
3. Arnaout A, Varela NP, Allarakhia M et al (2020) Baseline staging imaging for distant metastasis in women with stages I, II, and III breast cancer. Curr Oncol. ;27(2):e123-e145. 10.3747/co.27.6147. PMID:32489262
4. Groheux D, Hindie E, Delord M et al (2016) 18F-FDG PET/CT for staging and restaging of breast cancer. J Nucl Med 57(Suppl 1):17S–26S. 10.2967/jnumed.115.157859PMID:26834096
5. Boellaard R, Delgado-Bolton R, Oyen WJG et al (2015) FDG PET/CT: EANM procedure guidelines for tumour imaging: version 2.0. Eur J Nucl Med Mol Imaging 42(2):328–354. 10.1007/s00259-014-2961-xPMID:25452219
6. Wen W, Xuan D, Hu Y et al (2019) Prognostic value of maximum standard uptake value, metabolic tumor volume, and total lesion glycolysis of positron emission tomography/computed tomography in patients with breast cancer: A systematic review and meta-analysis. PLoS One. ;14(12):e0225959. 10.1371/journal.pone.0225959. PMID:31826010
7. Young H, Baum R, Cremerius U et al (1999) Measurement of clinical and subclinical tumour response using [18F]-fluorodeoxyglucose and positron emission tomography: review and 1999 EORTC recommendations. Eur J Cancer 35(13):1773–1782. 10.1016/S0959-8049(99)00229-4PMID:10673991
8. Wahl RL, Jacene H, Kasamon Y, Lodge MA (2009) From RECIST to PERCIST: Evolving considerations for PET response criteria in solid tumors. J Nucl Med 50(Suppl 1):122S–150S. 10.2967/jnumed.108.057307PMID:19403881

9. Lambin P, Leijenaar RTH, Deist TM et al (2017) Radiomics: the bridge between medical imaging and personalised medicine. Nat Rev Clin Oncol. ;14(12):749–762. 10.1038/nrclinonc.2017.141. PMID:28975929
10. Aerts HJWL, Velazquez ER, Leijenaar RTH et al (2014) Decoding tumour phenotype by noninvasive imaging using a quantitative radiomics approach. Nat Commun 5:4006. 10.1038/ncomms5006PMID:24892406
11. Ha S, Choi H, Paeng JC, Cheon GJ (2019) Radiomics in oncological PET/CT: a methodological overview. Nucl Med Mol Imaging 53(1):14–29. 10.1007/s13139-019-00571-4PMID:30828395
12. Zwanenburg A, Vallières M, Abdalah MA et al (2020) The Image Biomarker Standardisation Initiative: standardized quantitative radiomics for high-throughput image-based phenotyping. Radiology 295(2):328–338. 10.1148/radiol.2020191145PMID:32154773
13. Apostolova I, Rogasch J, Steffen IG et al (2014) Asphericity of pretherapeutic tumor FDG uptake in primary non-small cell lung cancer: a new prognostic marker. BMC Cancer 14:896. 10.1186/1471-2407-14-896PMID:25444154
14. Apostolova I, Steffen IG, Wedel F et al (2014) Asphericity of pretherapeutic tumor FDG uptake provides independent prognostic value in head-and-neck cancer. Eur Radiol 24(9):2077–2087. 10.1007/s00330-014-3269-8PMID:24965509
15. Groheux D, Martineau A, Teixeira L et al (2017) 18F-FDG PET/CT for predicting the outcome in ER+/HER2- breast cancer patients: comparison of clinicopathological parameters and PET image-derived indices including tumor texture analysis. Breast Cancer Res 19:3. 10.1186/s13058-016-0793-2PMID:28057031
16. Wasserthal J, Breit HC, Meyer MT, Pradella M, Hinck D, Sauter AW et al (2023) TotalSegmentator: Robust segmentation of 104 anatomic structures in CT images. Radiol Artif Intell 5(5):e230024. 10.1148/ryai.230024PMID:37795137
17. Isensee F, Jaeger PF, Kohl SAA, Petersen J, Maier-Hein KH (2021) nnU-Net: a self-configuring method for deep learning-based biomedical image segmentation. Nat Methods 18(2):203–211. 10.1038/s41592-020-01008-zPMID:33288961
18. Semenza GL (2012) Molecular mechanisms mediating metastasis of hypoxic breast cancer cells. Trends Mol Med. ;18(9):534–543. 10.1016/j.molmed.2012.08.001. PMID:22921864
19. Hanahan D, Weinberg RA (2011) Hallmarks of cancer: the next generation. Cell. ;144(5):646–674. 10.1016/j.cell.2011.02.013. PMID:21376230
20. Vickers AJ, Elkin EB (2006) Decision curve analysis: a novel method for evaluating prediction models. Med Decis Mak 26(6):565–574. 10.1177/0272989X06295361PMID:17099194
21. Groheux D, Sanna A, Majdoub M et al (2015) Baseline tumor 18F-FDG uptake and modifications after 2 cycles of neoadjuvant chemotherapy are prognostic of outcome in ER+/HER2- breast cancer. J Nucl Med 56(6):824–831. 10.2967/jnumed.115.154138PMID:25883123
22. Antunovic L, De Sanctis R, Cozzi L et al (2019) PET/CT radiomics in breast cancer: promising tool for prediction of pathological response to neoadjuvant chemotherapy. Eur J Nucl Med Mol Imaging

46(7):1468–1477. 10.1007/s00259-019-04313-8PMID:30915523

23. Ha S, Park S, Bang JI, Kim EK, Lee HY (2017) Metabolic radiomics for pretreatment 18F-FDG PET/CT to characterize locally advanced breast cancer: histopathologic characteristics, response to neoadjuvant chemotherapy, and prognosis. Sci Rep 7(1):1556. 10.1038/s41598-017-01524-7PMID:28484211
24. Roy S, Whitehead TD, Li S, Ademuyiwa FO, Wahl RL, Dehdashti F, Shoghi KI (2022) Co-clinical FDG-PET radiomic signature in predicting response to neoadjuvant chemotherapy in triple-negative breast cancer. Eur J Nucl Med Mol Imaging. ;49(2):550–562. 10.1007/s00259-021-05489-8. PMID:34328530. Erratum in: Eur J Nucl Med Mol Imaging. 2022;49(2):788. doi:10.1007/s00259-021-05542-6. PMID:34550428
25. Chen K, Wang J, Li S et al (2023) Clinical utility of a multi-scanner radiomics model based on 18F-FDG PET/CT for predicting neoadjuvant chemotherapy efficacy in breast cancer: development and external validation. Eur J Nucl Med Mol Imaging 50(7):1869–1880. 10.1007/s00259-023-06150-2PMID:36808002
26. Jung JH, Son SH, Kim DH et al (2017) Independent prognostic value of asphericity of pretherapeutic F-18 FDG uptake by primary tumors in patients with breast cancer. Med (Baltim) 96(46):e8438. 10.1097/MD.0000000000008438PMID:29145250
27. Cegla P, Hofheinz F, van den Hoff J et al (2023) Asphericity derived from [18F]FDG PET as a new prognostic parameter in cervical cancer patients. Sci Rep 13:8423. 10.1038/s41598-023-35191-8PMID:37225735
28. Hausmann P, Sura R, Zschaeck S et al (2025) Tumor asphericity in FDG PET is an independent prognostic parameter improving risk stratification in patients with head and neck squamous cell carcinoma. J Nucl Med 66(5):686–691. 10.2967/jnumed.124.268972PMID:40081960
29. Han S, Choi JY (2020) Prognostic value of 18F-FDG PET and PET/CT for assessment of treatment response to neoadjuvant chemotherapy in breast cancer: a systematic review and meta-analysis. Breast Cancer Res 22(1):119. 10.1186/s13058-020-01350-2PMID:33129348

Figures

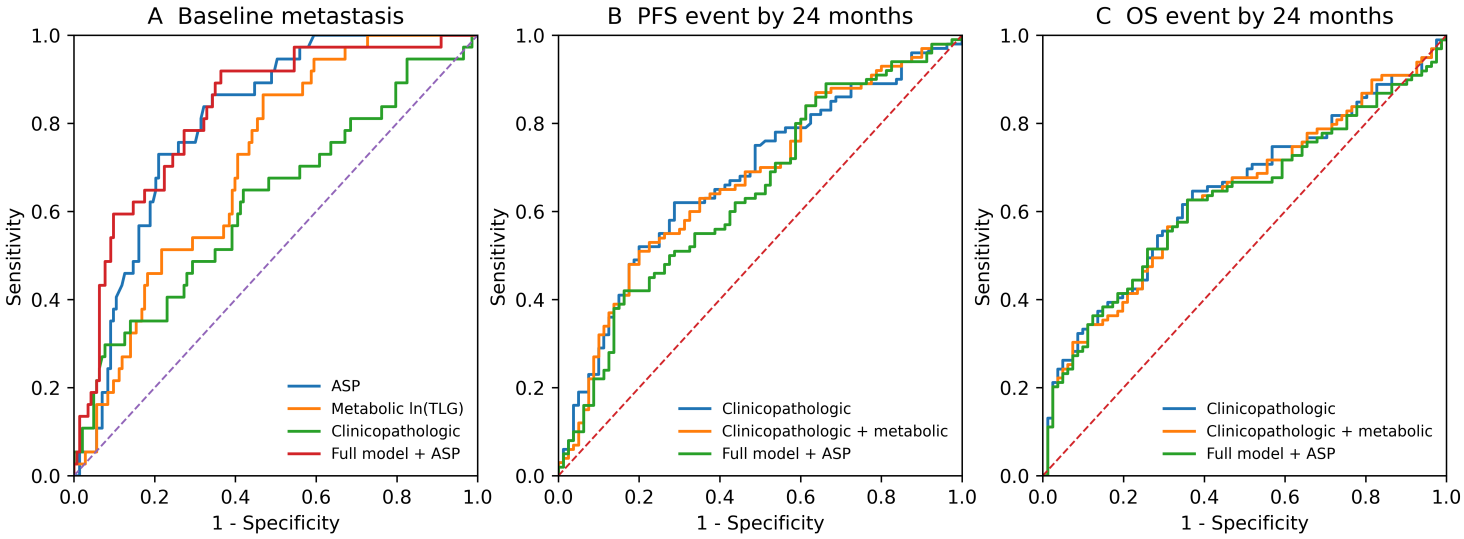


Figure 1

Fig1. Receiver operating characteristic (ROC) curves for prediction of baseline metastatic disease and 24 month outcomes using baseline FDG tumour asphericity (ASP) and multivariable models. (A) Baseline distant metastasis at presentation: AUC 0.80 for ASP alone, 0.71 for metabolic model (ln[TLG]), 0.62 for clinicopathologic model, and 0.82 for full model including ASP. (B) 24 month progression free survival (PFS) event: AUC 0.67 for clinicopathologic model, 0.66 for clinicopathologic plus metabolic model, and 0.64 for full model including ASP. (C) 24 month overall survival (OS) event: AUC 0.64 for clinicopathologic model, 0.64 for clinicopathologic plus metabolic model, and 0.63 for full model including ASP.

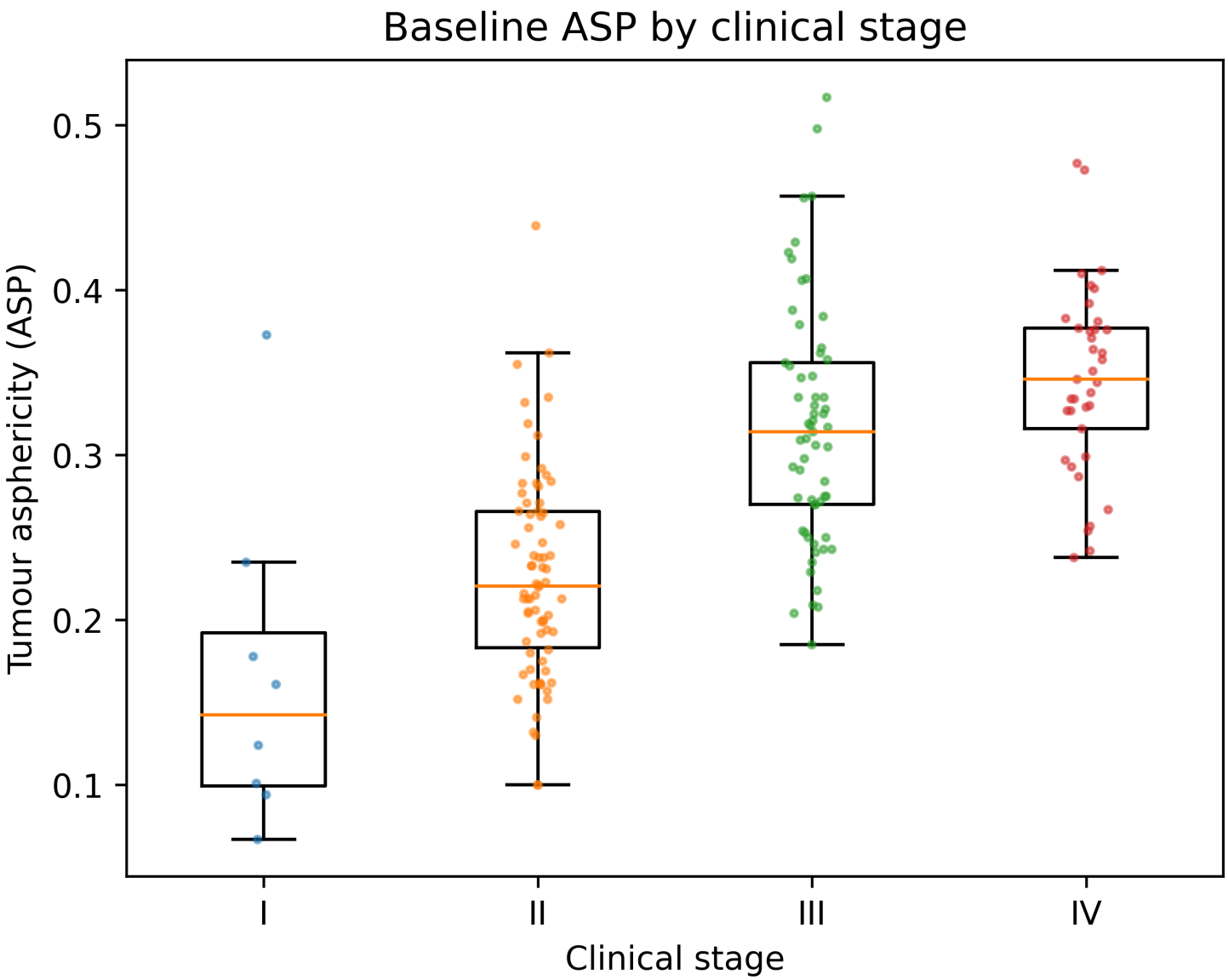


Figure 2

Figure 2. Distribution of baseline tumour asphericity (ASP) by clinical stage. ASP increased stepwise with advancing stage (median [IQR] stage I: 0.143 [0.099-0.192], stage II: 0.221 [0.183-0.266], stage III: 0.314 [0.270-0.356], stage IV: 0.346 [0.316-0.377]; Kruskal-Wallis p<0.001).

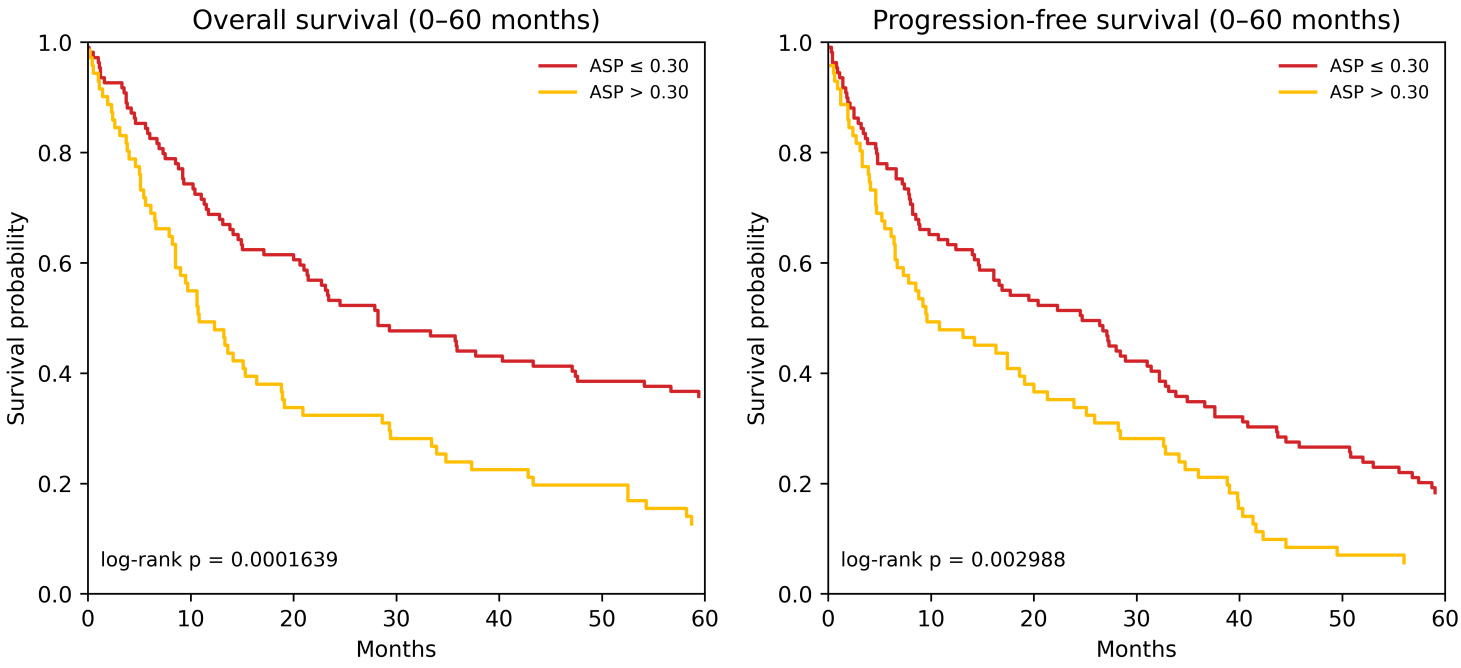


Figure 3

Figure 3. Kaplan-Meier survival curves stratified by tumour asphericity (ASP >0.30 vs ASP ≤0.30) for the overall cohort, with curves administratively censored at 60 months. Left: overall survival. Right: progression free survival. High asphericity is shown in yellow and low asphericity in red; log-rank p values are shown in each panel. Median OS was 28.2 months (ASP ≤0.30; n=109) versus 10.8 months (ASP >0.30; n=71) (log-rank p = 0.00016). Median PFS was 24.7 months (ASP ≤0.30) versus 9.6 months (ASP >0.30) (log-rank p = 0.0030).

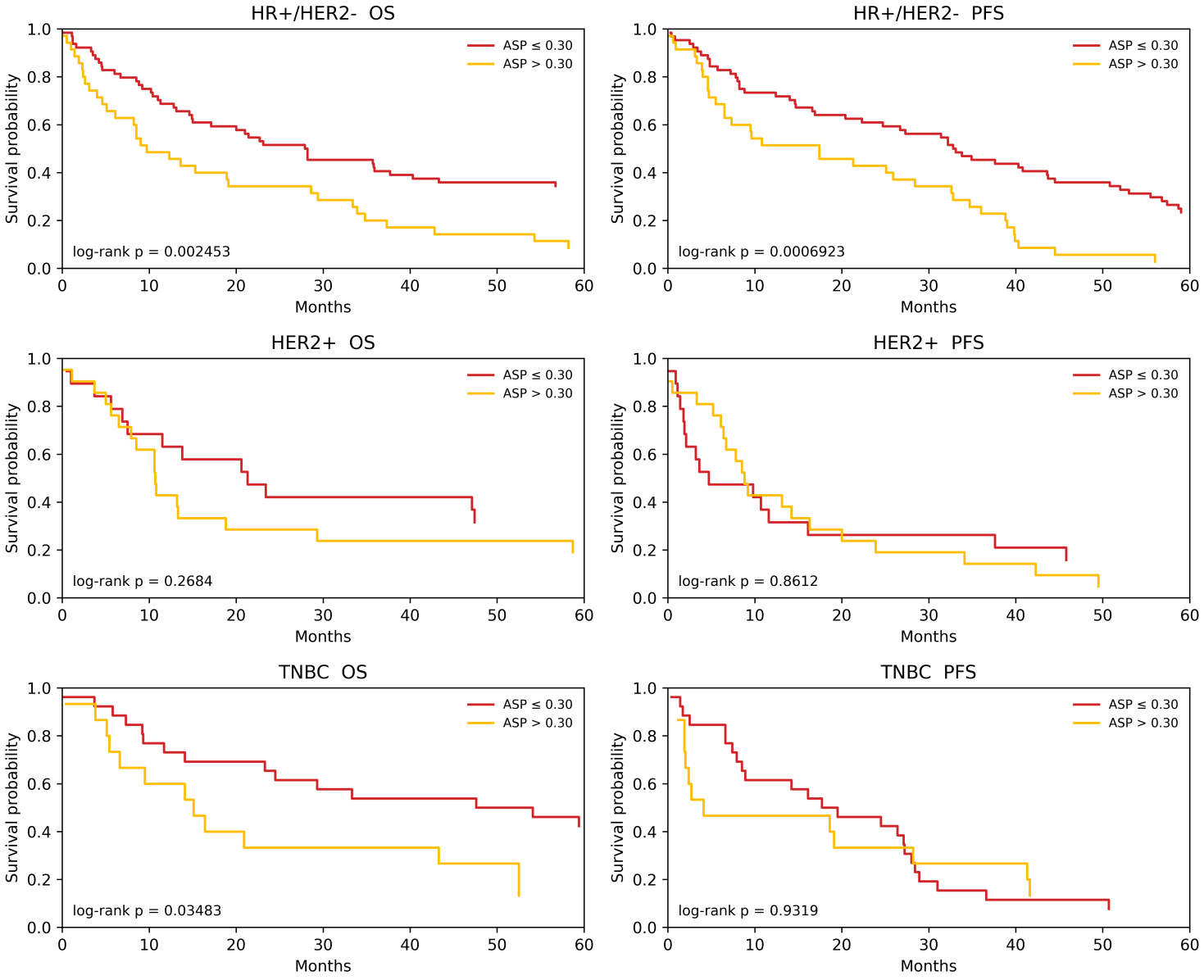


Figure 4

Figure 4. Kaplan-Meier survival curves stratified by tumour asphericity (ASP >0.30 vs ASP ≤0.30) within molecular subtypes, with curves administratively censored at 60 months. Top row: HR+/HER2- (n=99); middle row: HER2+ (n=40); bottom row: triple negative breast cancer (n=41). Left column: overall survival; right column: progression free survival. Log-rank p values are shown in each panel; high asphericity is shown in yellow and low asphericity in red. Median OS (ASP >0.30 vs ASP ≤0.30) was 9.7 vs 27.9 months in HR+/HER2- (p = 0.0025), 10.7 vs 21.3 months in HER2+ (p = 0.268), and 15.1 vs 47.6 months in TNBC (p = 0.0348). Median PFS (ASP >0.30 vs ASP ≤0.30) was 17.4 vs 32.8 months in HR+/HER2- (p = 0.00069), 8.8 vs 4.7 months in HER2+ (p = 0.861), and 4.1 vs 17.7 months in TNBC (p = 0.932).in HR+/HER2- (p = 0.00069), 8.8 vs 4.7 months in HER2+ (p = 0.861), and 4.1 vs 17.7 months in TNBC (p = 0.932).

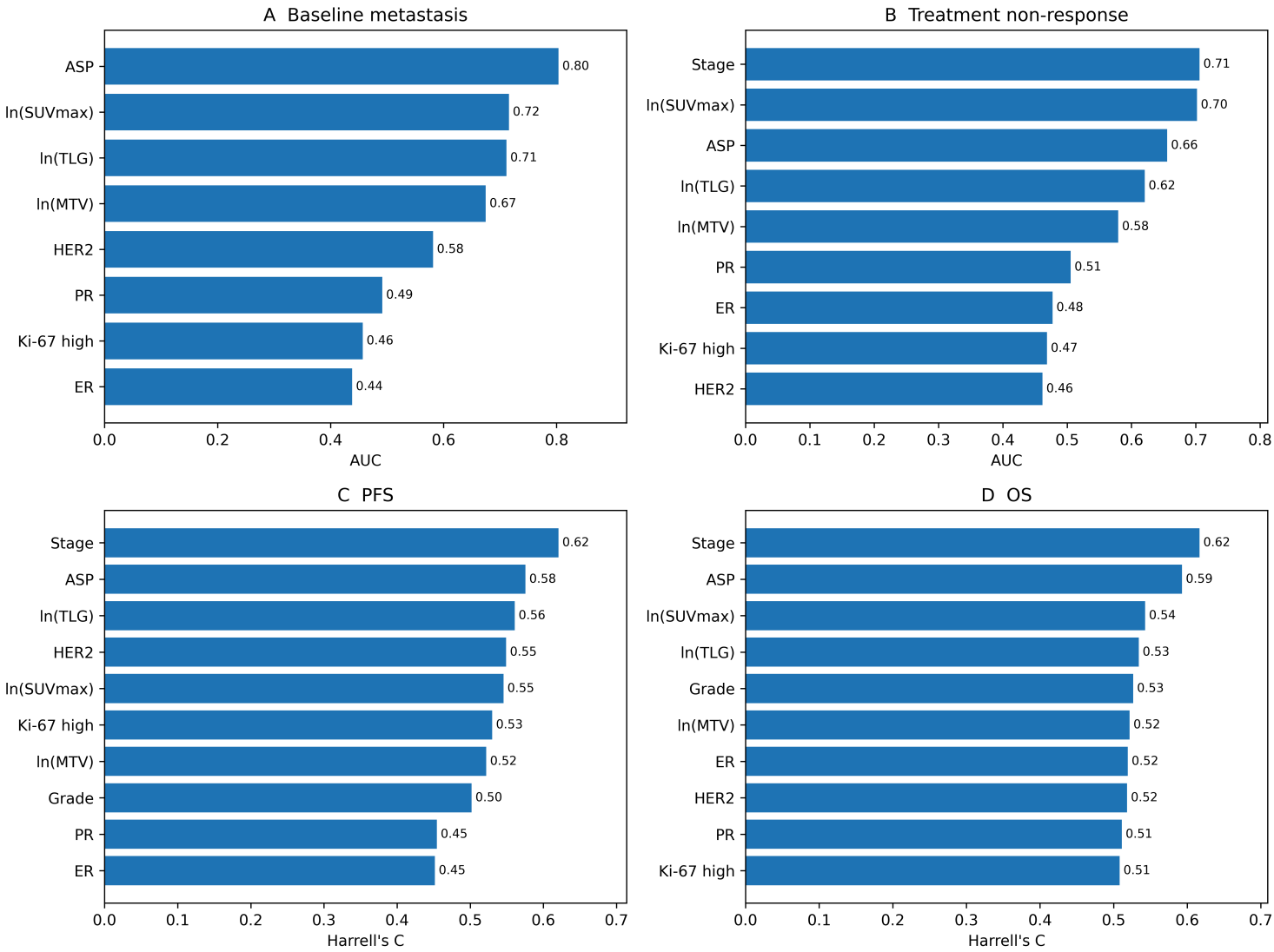


Figure 5

Figure 5. Comparative model discrimination of baseline FDG PET asphericity versus metabolic and biomarker variables for baseline metastasis, treatment non response, and survival. Baseline metastasis AUCs: ASP (per 0.1) 0.80, ln(SUVmax) 0.72, ln(TLG) 0.71, ln(MTV) 0.67, receptor and Ki-67 features ≤0.58. Treatment non response AUCs: stage 0.71, ln(SUVmax) 0.70, ASP (per 0.1) 0.66, ln(TLG) 0.62, ln(MTV) 0.58, others ≤0.54. Harrell's C for PFS and OS shows stage as the strongest predictor (0.62 for both) and ASP as the highest performing imaging biomarker (PFS 0.58; OS 0.59). ln denotes natural logarithm transformation.

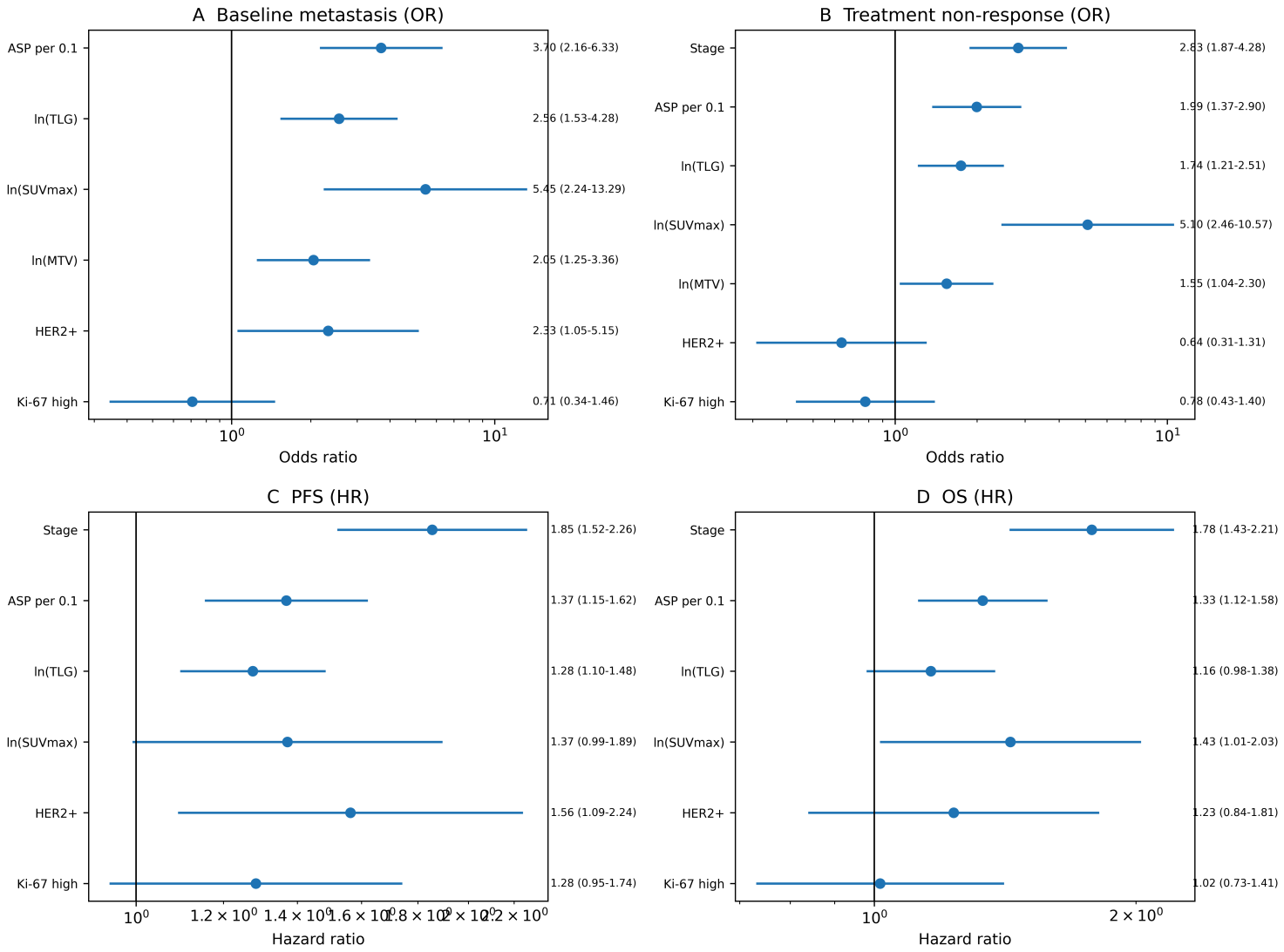


Figure 6

Figure 6. Univariable associations of FDG PET tumour asphericity (ASP), PET metabolic parameters, and receptor and Ki-67 status with baseline metastasis, treatment non response, and survival outcomes. Forest plots show odds ratios (OR) for baseline metastasis and treatment non response, and hazard ratios (HR) for PFS and OS, with 95% confidence intervals.

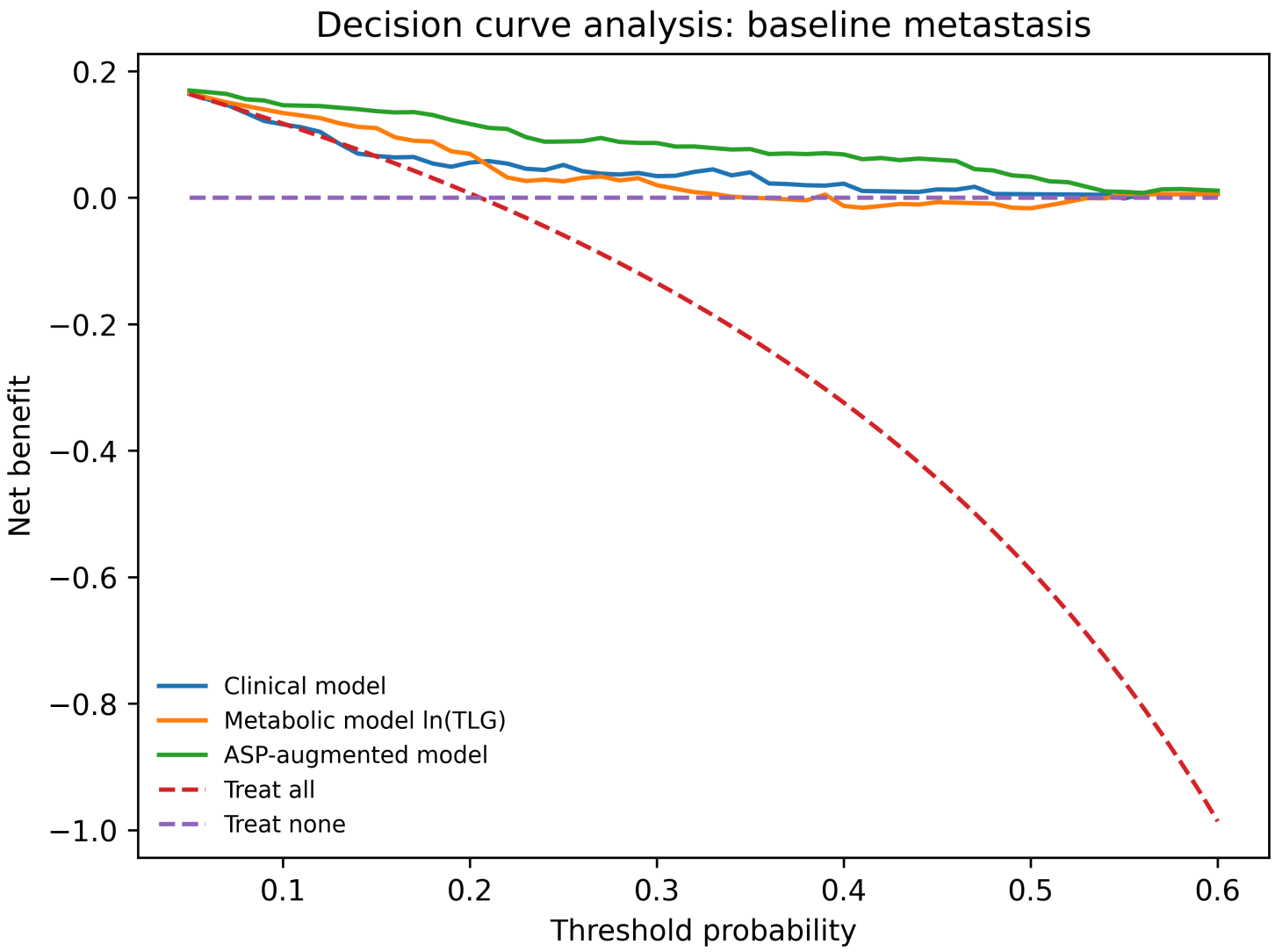


Figure 7

Figure 7. Decision curve analysis (DCA) for prediction of de novo metastatic disease at presentation. Net benefit is shown across threshold probabilities from 0.05 to 0.60 for the clinical model, metabolic model (ln[TLG]), and the ASP augmented model, alongside treat all and treat none strategies; higher curves indicate greater clinical utility.

Supplementary Files

This is a list of supplementary files associated with this preprint. Click to download.

- SupplementaryFigure.docx